Journal of The Electrochemical Society, **161** (4) H240-H243 (2014)
0013-4651/2014/161(4)/H240/4/$31.00 © The Electrochemical Society

Enhanced Photoelectrochemical Response of Silicon Nanowire Arrays through Coating the Carbon Shell

Shaolong Wu,[a,z] Xiaofeng Li,[a] Yaohui Zhan,[a] Jianhua Deng,[b] and Guo-an Cheng[c,z]

[a]*Institute of Modern Optical Technologies & Collaborative Innovation Center of Suzhou Nano Science and Technology, Key Lab of Advanced Optical Manufacturing Technologies of Jiangsu Province & Key Lab of Modern Optical Technologies of Education Ministry of China, Soochow University, Suzhou 215006, China*
[b]*College of Physics and Materials Science, Tianjin Normal University, Tianjin 300387, China*
[c]*Key Laboratory of Beam Technology and Material Modification of the Ministry of Education, College of Nuclear Science and Technology, Beijing Normal University, Beijing 100875, China*

Silicon nanowire array (SiNWs)-based photoelectrochemical (PEC) cells are regarded as a new and prospective candidate for optoelectronic applications due to their excellent optical absorption, large specific surface, and low-cost preparation. However, they suffer from the surface recombination of photocarriers and from photo-corrosion/photo-oxidation. In this work, the PEC response characteristics of SiNWs before and after covering with a thin carbon film were investigated. An enhancement factor of 35.87% in the PEC responsivity was observed after coating with the carbon shell. The degradations of the photocurrent with increasing illumination time and of the photocurrent versus potential with increasing measurement number were suppressed by the carbon shell.
© 2014 The Electrochemical Society. [DOI: 10.1149/2.089404jes] All rights reserved.

Manuscript submitted January 14, 2014; revised manuscript received February 14, 2014. Published February 19, 2014.

To obtain high performance from conventional photovoltaic devices arranged in a bulk formation, two fundamental requirements must be fulfilled, i.e., the photoactive layers must be thick enough to adequately absorb incident photons (especially for indirect-band materials like silicon (Si) and germanium (Ge)), and the minority-carrier diffusion length must be compatible with the large absorption depth (i.e., 125 μm thick Si is needed to absorb 90% of the above-bandgap photons), which means that the materials should be highly purified.[1,2] The simultaneous demands of high-quality crystalline materials and thick absorption layers inevitably give rise to a high production cost. However, one-dimensional (1D) nanostructures provide a promising and prospective approach to fabricate low-cost and high-performance optoelectronic devices owning to their large length-to-diameter and surface-to-volume ratios.[3–6] First, excellent light absorption can be realized from 1D nanostructure arrays with a small volume due to their moth-eye-like morphology perfect for antireflection effect[7,8] and light confinement under various optical mechanisms.[9–11] Second, the promising orthogonal spatial relation between carrier separation and photon absorption (via radial junction) guarantees a short diffusion distance and an effective carrier collection, allowing the low-grade materials to be available for high-performance optoelectronic devices.[1,2,12]

To fabricate solid-state and uniform radial junctions, complex instruments and harsh conditions are usually needed for in situ growth of the coaxial multishell 1D nanostructures.[13] The situation becomes even more severe if a radial junction with a specific doping requirement is involved.[14] In contrast, liquid-state radial junctions, which can be easily prepared via photoelectrochemical (PEC) cells,[15–17] emerge as a prototypical configuration for 1D nanostructure arrays in order to explore new concepts for solar energy applications. Nevertheless, two challenges still exist in achieving high-performance nanostructured devices based on liquid-state junctions. First, the nanostructure photoelectrodes in an electrolyte are generally degenerated significantly by photo-oxidation and/or photo-corrosion due to the large surface-to-volume ratio and high surface energy. Numerous efforts have been made to improve the PEC-behavior stability, e.g., using a non-corrosive organic salt presenting a liquid status instead of an aqueous electrolyte.[18] Second, the surface recombination loss is obvious,[19] especially for those nanostructures with rough surface topography prepared in a top-down method, which usually gives rise to large surface recombination velocity and a high surface trap density.[17] Previous reports have verified that surface passivation (or other surface treatments) is an effective route to lowering the surface recombination and improving the device performances.[20,21]

In our previous papers, morphology control of the Si nanowires (SiNWs) and the corresponding PEC properties were systematically investigated.[12,17,22] We concluded the PEC responses of SiNWs are strongly dependent on their surface morphology and that the overall PEC stability is relatively poor. This article presents a potential method for improving the PEC stability and responsivity, i.e., through a core-shell design based on our special surface treatment technique. First, vertically aligned SiNWs were produced by metal-assisted chemical etching (MacE). Then, the Si-core/carbon-shell nanowire arrays were obtained via deposition of a uniform carbon film on the as-prepared SiNWs by microwave plasma-enhanced chemical vapor deposition (MW-PECVD). Experimental results verify that the chemically stable carbon shell can well passivate the SiNW surfaces and protect them against photo-oxidation; therefore, the PEC-response stability and the PEC responsivity of silicon nanowire arrays in aggressive aqueous HBr/Br_2 electrolyte under yellow light irradiation can be substantially improved. Our design is expected to provide a way for realizing high-performance 1D nanostructured optoelectronic devices.

Experimental

Vertically aligned SiNWs were fabricated by MacE from n-type Si (100) wafers with the resistivity of 2–2.7 Ω · cm. The fabrication contains four main steps summarized as follows (refer to our previous report[22] for details). Ultrasonically clean the cut Si chips in deionized water, acetone and ethanol for 10 min in sequence, and then boil them in H_2SO_4/H_2O_2 (4:1 by volume) solution for 15 min. Dip the as-cleaned Si chips into HF dilute solution for 2 min to remove the silicon oxide layer and then immerse them into the aqueous solution mixed with 4.8 M HF and 0.01 M $AgNO_3$ for 1 min to deposit Ag nanoparticles (AgNPs). Soak the AgNP-coated Si chips in the aqueous solution mixed with 4.0 M HF and 0.2 M H_2O_2 for 10 min. Remove the residual AgNPs of the as-etched SiNWs with 50% HNO_3. All of the chemical reagents were analytical grade and all of these operations were carried out at room temperatures (20−25°C).

A uniform carbon film was deposited by MW-PECVD with the following main coating conditions:[23] C_2H_2 flow of 2 sccm, H_2 flow of 20 sccm, MW power of 400 W, background temperature of 700°C, background pressure of 1 kPa, and a deposition time of 60 min.

The morphological and structural characterizations of the as-prepared and carbon-film-covered SiNWs were examined by a field-emission scanning electron microscope (FE-SEM S-4800, Hitachi) and a high-resolution transmission electron microscope (HR-TEM, JEM-2010, JEOL). Raman spectroscopy was measured by laser resonance Raman spectroscopy with 633 nm excitation-wave (LobRAM, ARAMIS) to characterize the carbon film. X-ray photoelectron

[z]E-mail: shaolong_wu@suda.edu.cn; gacheng@bnu.edu.cn

Downloaded on 2014-07-12 to IP 59.64.60.107 address. Redistribution subject to ECS terms of use (see ecsdl.org/site/terms_use) unless CC License in place (see abstract).

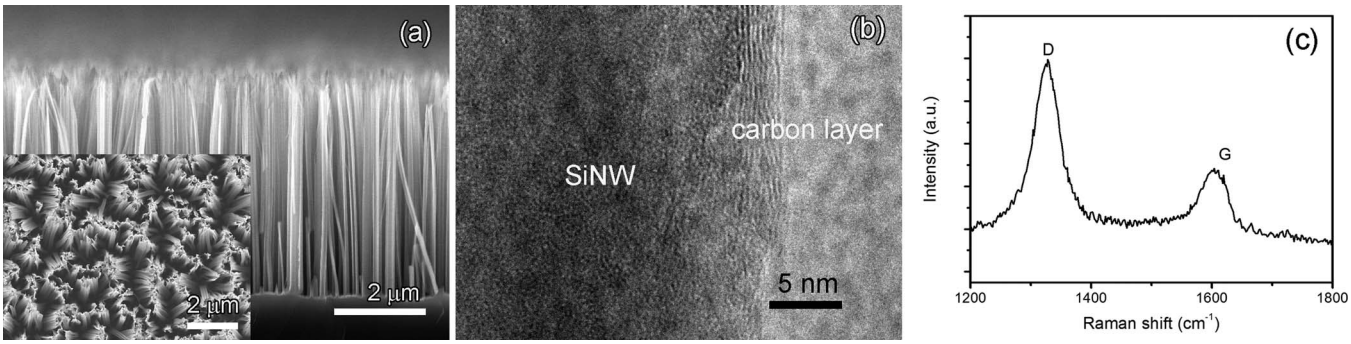

Figure 1. (a) Cross-sectional SEM of the SiNWs coated by carbon-film shell (C/SiNWs). Inset: corresponding top-view SEM image. (b) HRTEM image of the edge of C/SiNWs. (c) Raman spectrum recorded from the top region of C/SiNWs.

spectroscopy (XPS, PHI-5300 ESCA) was used to characterize the chemical bonding states of the Si element before and after the PEC measurements.

Measurements of the PEC response were performed by two steps. First, SiNW photoelectrodes were prepared by sputtering a ∼1 μm thick Al layer with on the back of the SiNWs. Post-annealing was conducted at 800°C for 30 min in a furnace under H_2 atmosphere. Second, the PEC cells were formed using the as-prepared photoelectrodes in a two-electrode configuration, where a Pt mesh was used as a counter electrode and a reference electrode (schematic of the PEC cell can be found elsewhere).[17] An electrochemical workstation (CS300, WUHAN Corrtest Instrument Co. Ltd.), a homemade electrolytic cell with a transparent quartz window, and a LED light irradiation system (SHENZHEN LTWG Electronics Co. Ltd.) were involved. All of the potential values in this work were with respect to the Pt electrode. The irradiation source was a yellow LED light with a wavelength range of 590−595 nm and an irradiation intensity of ∼41.75 Wm^{-2} as measured by a commercial Si photodetector (DSi200, UV-100L, BEIJING Zolix Instrument Co. Ltd.). The active area of the photoelectrodes was approximately 1.227 cm^2. The electrolyte solution was a mix of 40 wt% HBr and 3 wt% Br_2 (4:1 by volume).

Results and Discussion

The typical morphology of the SiNWs with carbon-film shell (C/SiNWs) is shown in Fig. 1a. The SiNWs are vertically aligned to the substrate, exhibiting a good uniformity in NW length (∼4.7 μm). The cross-section shapes are, however, relatively non-uniform, despite the NW diameters being mostly between 80 and 300 nm, as previously demonstrated.[12,17,22] The specific SiNW morphological characteristics can be ascribed to the non-patterned AgNP catalysts with random distribution;[22,24] moreover, the etching conditions also play an indispensable role in determining the morphology of the resultant SiNWs. The detailed analysis of the condition effects and the corresponding fabrication mechanism has been extensively addressed in our previously.[22] Considering that the carbon film is very thin and hard to see in the SEM images, HRTEM analysis was used to certify the existence of the carbon film. As shown in Fig. 1b, a thin carbon film (3–4 nm thick) is located on the SiNW surfaces. We measured the Raman spectrum to further identify the carbon film. Figure 1c shows two Raman peaks centered around 1327 and 1602 cm^{-1}, which are related to disordered carbon (D-band) and the graphite carbon (G-band), respectively.[25] The integral intensity ratio of the D-to-G peaks is 3.25, indicating that the disordered carbon dominates in the deposited carbon film. Observations of carbon atom layers and Raman characteristic peaks of the carbon element confirm that the carbon-shell/Si-core NW arrays were successfully prepared.

Measuring the open-circuit potential (OCP) is a convenient method for estimating the corrosion resistance of the electrode in an electrolyte.[26–28] Figure 2 plots OCP as a function of measuring time under an 80 sec pulse of illumination in HBr/Br_2 electrolyte. Before the illumination, the OCP of the SiNWs (−0.097 V) is more negative than that of the C/SiNWs (−0.009 V), which means that the stability of the surface states of SiNWs (i.e., corrosion resistance) is improved by a carbon shell coating from the viewpoint of thermodynamics. Under a pulse illumination, the OCP of both samples simultaneously dropped to much more negative values; however, compared to the bare SiNWs, the photo-OCP of the C/SiNWs is always higher, exhibiting a

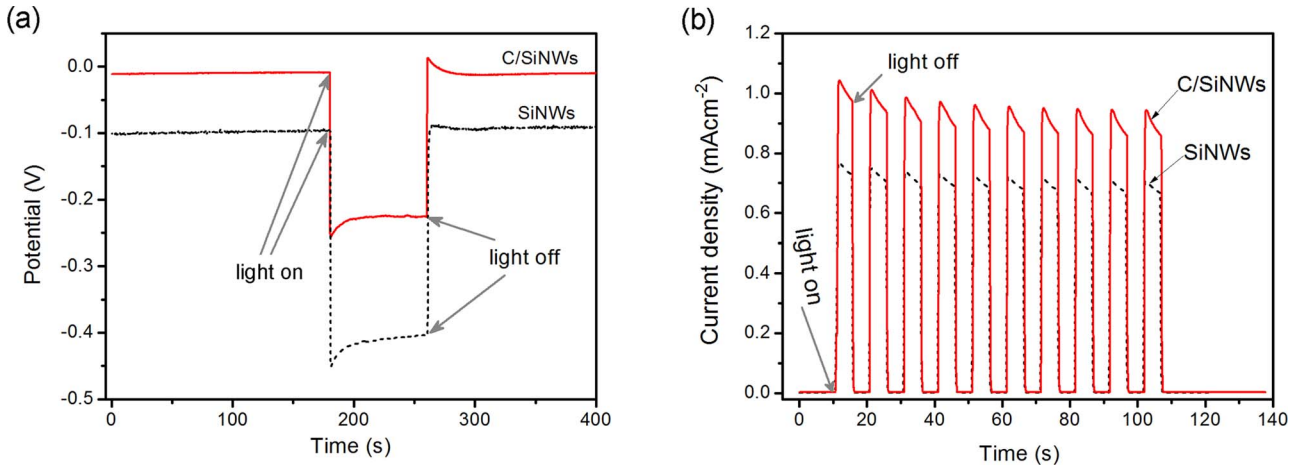

Figure 2. (a) Open-circuit potential versus measuring time of SiNWs and C/SiNWs under an 80 sec pulse of illumination. (b) Current density versus measuring time of SiNWs and C/SiNWs under ON−OFF cycle illumination at 1.0 V potential.

Downloaded on 2014-07-12 to IP 59.64.60.107 address. Redistribution subject to ECS terms of use (see ecsdl.org/site/terms_use) unless CC License in place (see abstract).

faster speed to the steady state. The OCP variations under the pulsed illumination highlight two important inferences: the illumination can deteriorate the corrosion resistance of both samples, in other words, photocorrosion very likely occurs in this condition, the corrosion resistance of the C/SiNWs is better than the bare SiNWs for both dark and illumination situations. Note, however, that under an illumination pulse the potential drop in the C/SiNWs (∼0.24 V) is smaller than that in the bare SiNWs (∼0.44 V), i.e., the carbon coating will give rise to a lower open-circuit voltage, making them undesirable for solar cell applications.

Photosensitivity measurements were performed to assess the passivation effect of the carbon shell. To ensure that all photogenerated carriers escaping from surface/bulk recombination can contribute to the photocurrent, 1.0 V potential was applied to the system when measuring the current under ON-OFF cycle illumination. As shown in Fig. 2b, both samples exhibited obvious PEC responses, with a much larger photocurrent from the C/SiNWs. The dark currents are very low for both samples due to the rectification effect in a reversely biased n-type semiconductor electrode.[12,29] Photoresponsivity (R, defined by the ratio of net photocurrent density and incident light power density)[12,17] of the SiNWs is enhanced from 0.184 to 0.250 AW^{-1} after depositing the carbon shell. An enhancement factor of 35.87% in R is a good indication that the carbon shell can indeed effectively suppress the surface recombination of SiNWs.

Photocurrent density as a function of potential (J-V curve) was measured by using linear sweep voltammetry from −1.5 to 2.0 V at an increment rate of 25 mVs^{-1}. Under steady-state illumination, we repeat the measurement for a number of times. The first and tenth J-V curves are shown in Fig. 3a, which exhibits two observations in

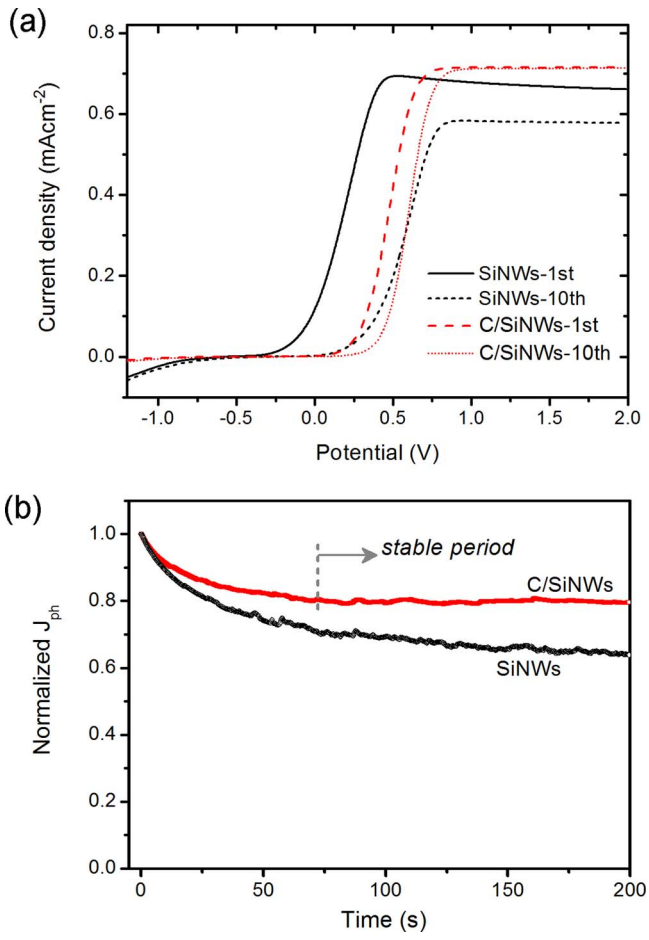

Figure 3. (a) Current density versus potentail of SiNWs and C/SiNWs under steady-state illumination for the first and tenth measurements. (b) Normalized photocurrent (J_{ph}) versus illumination time measured at 1.0 V potential.

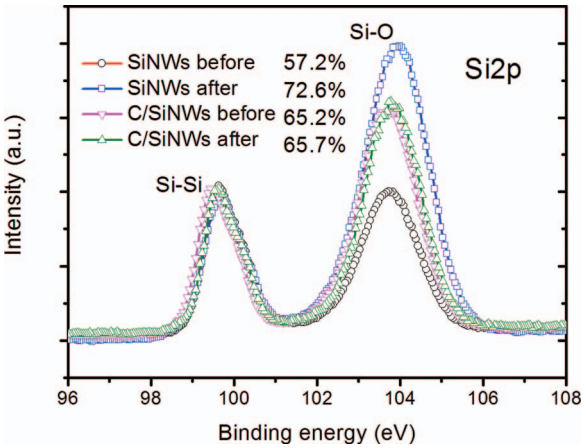

Figure 4. Normalized XPS spectra of SiNWs and C/SiNWs before and after PEC measurements. These percentage numbers are the corresponding ratios of Si-O covalent bonds to all the Si chemical states.

common with increasing measurement number, i.e., the J-V curves shift toward the higher potentials, and the current densities are decreased. However, after repeating the measurement ten times, the saturation photocurrent (J_{sp}, the maximal photocurrent) for bare SiNWs decreases from 0.693 to 0.582 $mAcm^{-2}$ and the corresponding saturation potential (V_{sp}, the potential corresponding to J_{sp}) increases from 0.503 to 0.884 V. In contrast, the J_{sp} decline for the C/SiNWs is slight and the increment of V_{sp} is just ∼0.1 V. Because the original oxidation layer of the bared SiNWs is thin, an obviously more positive V_{sp} of C/SiNWs relative to that of bare SiNWs for the first measurement can be attributed to the carbon shell, which improves the barrier height of the photocarriers passing through the Si-electrolyte interfaces. However, as scan times increase, the thickness of the oxidation layer of the bared SiNWs is gradually increased, while that of the C/SiNWs is limited. Therefore, the V_{sp} of the bared SiNWs is close to that of the C/SiNWs for the tenth measurement.

Photocurrent stability was further evaluated by measuring the photocurrent as a function of illumination time. For an easy comparison, the photocurrent was normalized according to the beginning value. Figure 3b shows that both samples suffer from rapid degradation within the first 30 s (i.e., a drop of ∼20.0% for the C/SiNWs and of ∼27.3% for the bare SiNWs). The drop for the bare SiNWs is conspicuous during the whole illumination time, while the photocurrent of the C/SiNWs reaches a relative stable status after 70 s. Degradation ratios of ∼20.5% for the C/SiNWs and of ∼36.1% for the bare SiNWs after 200 s illumination are observed from the experiments. The bare SiNWs with poor stability performance are mainly caused by the deleterious photo-corrosion/photo-oxidation reaction undergone by the nanostructured silicon electrode contacting with an aqueous electrolyte.[18,20] The depicted stability clearly attests that the carbon shell coating can improve resistance against photo-corrosion and photo-oxidation.

To further analyze the carbon film effect in the SiNW PEC response, we measured the XPS spectra of both samples before and after PEC tests to probe the chemical states of Si element of SiNW surfaces. Figure 4 is the Si2p peaks of XPS spectra, displaying two peaks at 99.6 and 103.8 eV, respectively. The former peak can be assigned to Si-Si covalent bonds, and the latter to Si-O covalent bonds.[30,31] The proportion of Si-O covalent bonds to all the Si chemical states can be estimated by calculating the integral intensity ratio of the two peaks. Calculations show that the SiO_x formation is dramatically suppressed by the carbon shell, while the Si-O band percentage for the bare SiNWs has a dramatic enhancement (i.e., from 57.2% to 72.6%) during the PEC response measurements. Note that the Si-O band percentages of all of the samples are relatively large, which can be ascribed to the combined actions of the ultra-large specific surfaces of SiNWs and the limited detection depth of XPS. XPS analysis certifies that the bare

Downloaded on 2014-07-12 to IP 59.64.60.107 address. Redistribution subject to ECS terms of use (see ecsdl.org/site/terms_use) unless CC License in place (see abstract).

SiNWs are extremely vulnerable to photo-oxidation in the aggressive HBr/Br_2 electrolyte, and the carbon film effectively protects the SiNW surfaces from photo-oxidation/photo-corrosion.

Conclusions

The SiNWs-core/carbon-shell hybrids were successfully fabricated through coating a uniform and thin carbon film with MW-PECVD technology onto the vertically aligned SiNWs prepared by MacE. The carbon shell not only prevents the formation of a thick insulating oxide layer and SiNW photo-corrosion but also suppresses the charge recombination at the SiNW surfaces. The corrosion resistance in HBr/Br_2 electrolyte, photoresponsivity and PEC-response stability of the SiNWs are substantially improved by depositing a carbon-film shell. However, the extraction of photocarriers between the SiNW-electrolyte interfaces is weakly hindered by introducing the carbon film, resulting in a higher saturation potential and a lower open-circuit voltage for solar cell applications. Further improvements of the PEC performances of SiNWs can be achieved by boosting the quality of carbon-film shell, as well as functionalizing the SiNW surfaces, using a non-aggressive electrolyte and optimizing the intrinsic properties of SiNWs.

Acknowledgments

This work was supported by the National Basic Research Program of China (2010CB832905), Ph.D. Programs Foundation of Ministry of Education of China (20133201110021), National Natural Science Foundation of China (No. 61204066, No. 91233119), "Thousand Young Talents Program" of China, and the Priority Academic Program Development (PAPD) of Jiangsu Higher Education Institutions.

References

1. B. M. Kayes, *Radial pn junction, wire array solar cells* [D], p. 5−12, California Institute of Technology, Pasadena, California (2009).
2. B. M. Kayes, H. A. Atwater, and N. S. Lewis, *J. Appl. Phys.*, **97**, 114302 (2005).
3. R. Q. Zhang, X. M. Liu, Z. Wen, and Q. Jiang, *J. Phys. Chem. C*, **115**, 3425 (2011).
4. A. P. Goodey, S. M. Eichfeld, J. M. Redwing, K. K. Lew, and T. E. Mallouk. *J. Am. Chem Soc.*, **129**, 12344 (2007).
5. G. B. Yuan, H. Z. Zhao, X. H. Liu, Z. S. Hasanali, Y. Zou, A. Levine, and D. W. Wang, *Angew. Chem. Int. Ed.*, **48**, 9680 (2009).
6. A. I. Hochbaum and P. D. Yang, *Chem. Rev.*, **110**, 527 (2010).
7. P. B. Clapham and M. C. Hutley, *Nature*, **244**, 281 (1973).
8. S. J. Wilson and M. C. Hutley, *J. Mod. Opt.*, **29**, 993 (1982).
9. S. Wu, Z. Zhang, R. Zheng, and G. Cheng, *J. Korean. Phys. Soc.*, **63**, 1189 (2013).
10. L. Cao, J. S. White, J.-S. Park, J. A. Schuller, B. M. Clemens, and M. L. Brongersma, *Nature Mater.*, **8**, 643 (2009).
11. Y. Yu and L. Cao, *Opt. Express*, **20**, 13847 (2012).
12. S. Wu, T. Zheng, R. Zheng, and G. Cheng, *Chem. Phys. Lett.*, **538**, 102 (2012).
13. J. D. Christesen, X. Zhang, C. W. Pinion, T. A. Celano, C. J. Flynn, and J. E. Cahoon, *Nano Lett.*, **12**, 6024 (2012).
14. K. Q. Peng, X. Wang, L. Li, X. L. Wu, and S.-T. Lee, *J. Am. Chem. Soc.*, **132**, 6872 (2010).
15. K. Q. Peng, X. Wang, and S.-T. Lee, *Appl. Phys. Lett.*, **92**, 163103 (2008).
16. G. Yuan, K. Aruda, S. Zhou, A. Levine, J. Xie, and D. Wang, *Angew. Chem. Int. Ed.*, **50**, 2334 (2011).
17. S. Wu, L. Wen, G. Cheng, R. Zheng, and X. Wu, *ACS Appl. Mater. Interfaces*, **5**, 4769 (2013).
18. X. Shen, B. Sun, F. Yan, J. Zhao, F. Zhang, S. Wang, X. Zhu, and S.-T. Lee, *ACS Nano*, **4**, 5869 (2010).
19. M. D. Kelzenberg, D. B. T-Evans, M. C. Putnam, S. W. Boettcher, R. W. Briggs, J. K. Baek, N. S. Lewis, and H. A. Atwater, *Energy Environ. Sci.*, **4**, 866 (2011).
20. X. Wang, K. Q. Peng, X. J. Pan, X. J. Chen, Y. Yang, L. Li, X. M. Meng, W. J. Zhang, and S.-T. Lee, *Angew. Chem., Int. Ed.*, **50**, 9861 (2011).
21. Y. Dan, K. Seo, K. Takei, J. H. Meza, A. Javey, and K. B. Crozier, *Nano Lett.*, **11**, 2527 (2011).
22. S. Wu, T. Zheng, R. Zheng, and G. Cheng, *Appl. Surf. Sci.*, **258**, 9792 (2012).
23. S. Wu, J. Deng, T. Zhang, R. Zheng, and G. Cheng, *Diamond Relat. Mater.*, **26**, 83 (2012).
24. Z. Huang, N. Geyer, P. Werner, J. Boor, and U. Gösele, *Adv. Mater.*, **23**, 285 (2011).
25. A. C. Ferrari, J. C. Meyer, V. Scardaci, C. Casiraghi, M. Lazzeri, F. Mauri, S. Piscanec, D. Jiang, K. S. Novoselov, S. Roth, and A. K. Geim, *Phys. Rev. Lett.*, **97**, 187401 (2006).
26. D. W. Deberry, *J. Electrochem. Soc.*, **132**, 1022 (1985).
27. C. Zhonga, N. T. Woodsb, G. B. Dawsonc, and M. D. Porter, *Electrochem. Commun.*, **1**, 17 (1999).
28. J. A. S. Roberts and R. M. Bullock, *Inorg. Chem.*, **52**, 3823 (2013).
29. M. Grätzel, *Nature*, **414**, 338 (2001).
30. H. Liu, G. Cheng, C. Liang, and R. Zheng, *Nanotechnol.*, **19**, 245606 (2008).
31. G. Cheng, F. Zhao, S. Wu, D. Zhao, J. Deng, R. Zheng, and Z. Ping, *J. Nanosci. Nanotechnol.*, **12**, 6543 (2012).

Downloaded on 2014-07-12 to IP 59.64.60.107 address. Redistribution subject to ECS terms of use (see ecsdl.org/site/terms_use) unless CC License in place (see abstract).